Dual-Band Metamaterial Based on Jerusalem Cross Structure With Interdigital Technique for LTE and WLAN Systems

W. KAMONSIN[ID]**1, P. KRACHODNOK**[ID]**1, (Member, IEEE), P. CHOMTONG**2**, (Member, IEEE), AND P. AKKARAEKTHALIN**3**, (Member, IEEE)**

1 School of Telecommunication Engineering, Institute of Engineering, Suranaree University of Technology, Nakhon Ratchasima 30000, Thailand
2 Department of Teacher Training in Electrical Engineering, Faculty of Technical Education, King Mongkut's University of Technology North Bangkok, Bangkok 10800, Thailand
3 Department of Electrical and Computer Engineering, Faculty of Engineering, King Mongkut's University of Technology North Bangkok, Bangkok 10800, Thailand

Corresponding author: P. Krachodnok (priam@sut.ac.th)

ABSTRACT This paper presents a novel metamaterial based on Jerusalem cross structure with interdigital technique to be applied for dual-band systems. The proposed structure can operate at resonant frequencies of 1.8 and 5.5 GHz for LTE and WLAN bands, respectively. The interdigital structure was added to connect at the end of the Jerusalem cross structure in order to control the resonant frequencies and to promote for permittivity adjustment. The proposed metamaterial unit cell was designed to achieve the simulated dual-band operation with bandwidths of 1.70 $\sim$ 1.95 GHz at 1.8 GHz and 5.06 $\sim$ 6.04 GHz at 5.5 GHz, respectively. The unit cell size is reduced from $\lambda/2$ to $\lambda/4$ which is much smaller than the conventional structure. The 5×5 unit cells of metamaterials were implemented as a reflector for a dipole antenna resulting in dual-band operation with bandwidths of 1.58 $\sim$ 1.88 GHz at 1.8 band and 5.05 $\sim$ 5.68 GHz at 5.5 band, respectively. Besides, the dipole antenna with the proposed metamaterial reflector has measured gains up to 8.23 dBi at 1.8 GHz and 8.30 dBi at 5.5 GHz, respectively. Moreover, the shape of metamaterial structure is symmetrical, so it can be used for dual linear polarization. Also, the antenna with the proposed reflector has low profile with the distance of $\lambda/8$ between radiator and reflector. Therefore, the proposed metamaterial can be applied for any antenna applicable for LTE and WLAN applications.

INDEX TERMS Dual-band, metamaterial, Jerusalem cross structure, interdigital.

I. INTRODUCTION

Nowadays, demand for wireless communication technology in LTE and WLAN systems is soaring, according to high internet usage growth. Therefore, there are needs for continuous improvement in data transmission and multi-frequency operation. Metamaterials have been popularly used in a variety of applications, especially to increase antenna performances in wireless communication systems [1]. Many researches have applied metamaterials to modify the electromagnetic properties [2] used in conjunction with antennas to increase efficiencies of transmitting and receiving signals.

The associate editor coordinating the review of this manuscript and approving it for publication was Wei E. I. Sha[ID].

They can be used as reflector [3], director [4], absorber [5], dielectric [6], etc. In previous researches on metamaterials, the unit cell was designed to be used for multi-frequency operation by using a double square ring structure [7]–[9]. In this design, the first and second resonant frequencies can be altered by adjusting the outer and inner ring parameters, respectively. However, the proposed metamaterial consists of many layers of materials, resulting in complicated structure. In [10], a triple-band resonator was employed for negative permittivity metamaterial operated in C-band and X-band. The unit cell consists of open delta structure within square ring. In addition, Jerusalem cross structure was presented in [11]. In this structure, the number of legs at the end must be increased in order to make multiple frequency
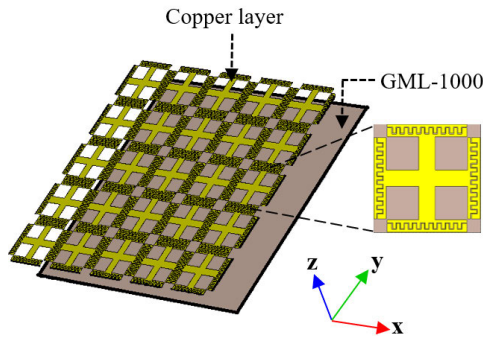
FIGURE 1. The proposed metamaterial and unit cell.

FIGURE 2. A dual-band metamaterial based on Jerusalem cross structure and interdigital part: (a) the equivalent circuit, (b) comparison the size between conventional structure and Jerusalem cross structure with interdigital part (c) the geometrical diagram of unit cell.

bands. However, the structures of the metamaterials as mentioned above are difficult to design, implement and modify, as results in restrictions on the use for antennas. Many techniques have been applied to create the metamaterials used for multi-frequency band operation. The unit cell with Jerusalem cross structure proposed in [12]–[14] is able to clearly adjust the frequency band but its structure has a length of $\lambda/2$ which is large and this technique can be used in E-plane and H-plane when connecting with antenna. Therefore, many researchers were interested in the interdigital technique to reduce the size of unit cell [15]–[17]. With the interdigital structure, the size of unit cell can be reduced from $\lambda/2$ to $\lambda/4$ [18], [19], which is the same electrical length. The interdigital connection at the end of unit cell structure will clearly affect the second resonant frequency adjustment, and it also affects the change of the permittivity of the metamaterial in which operating frequency has negative permittivity (ENG) [20], [21]. Therefore, in this research we propose to design a dual-band metamaterial used for LTE and WLAN systems at 1.8 GHz and 5.5 GHz frequency bands by using the Jerusalem cross structure with interdigital technique. The unit cell is designed with size reduction from $\lambda/2$ to $\lambda/4$ which is much smaller than the conventional structure. Also, the antenna with the reflector using the proposed unit cells has low profile with the distance of $\lambda/8$ between radiator and reflector. Moreover, it has linear polarization in both vertical and horizontal planes or dual polarization, and higher performances including higher gains in both of operated frequency bands. Details of the design will be shown in the next section. Then, the simulation of unit cell and measurement of the proposed structure will be shown and discussed in section 3. Finally, conclusions will be given.

II. DESIGN OF UNITCELL

The simple design of dual-band metamaterial, whose unit cell includes Jerusalem cross structure with interdigital part is shown in Fig. 1. The GML-1000 substrate with $\varepsilon_r = 3.2$, thickness of 0.762 mm, and loss tangent of 0.004, is employed. The unit cell is designed at the first resonant frequency of 1.8 GHz and the second resonant frequency of 5.5 GHz, respectively. The equivalent circuit of designed metamaterial unit cell is shown in Fig. 2(a). By modifying unit cell, the Jerusalem cross structure which includes the
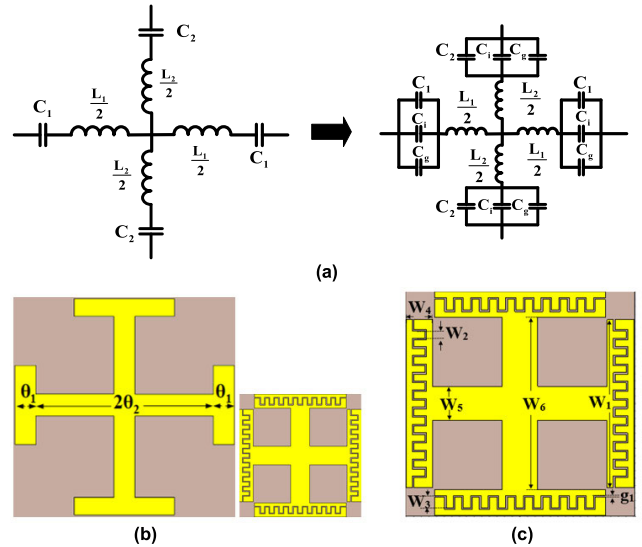
size of cross line and the capacitance of interdigital structure can reduce both resonant frequencies. In the circuit model, the inductors and capacitors are added caused by the interdigital structure. The adjustment in capacitance 'Ci' affects a significant shift in the second resonant frequency. The value of capacitance is increased by increasing the number of fingers of interdigital structure, thus the gaps between fingers involve with the increase in the E-field.

Fig. 2(b) also shows the impedance of the transmission line (Z_a) that affects the resonant frequency. By having the electrical length $\theta_a = 2(\theta_1 + \theta_2)$, where $\theta_1 = \theta_2 = \theta$, the stepped impedance of the transmission line can be determined by using (1)–(2), where f_1 and f_2 are the fundamental and second resonance frequencies, respectively. The electrical lengths can be derived as [22]–[25]:

$$\theta_{a0} = 2\tan^{-1}\left(\frac{1}{\pi f_1 Z_a C_i}\right) \tag{1a}$$

$$\theta_{a1} = 2\pi - 2\tan^{-1}(\pi f_2 Z_a C_i) \tag{1b}$$

The parameter Ci can be determined as

$$C_i = \frac{(\varepsilon_r + 1)}{W_1} W_3(\varepsilon_r + 1)[0.1(n - 3) + 0.11] \tag{2}$$

where θ_{a0} and θ_{a1} are the electrical lengths of the first and second resonance frequencies, respectively. Ci is the capacitance of the interdigital part, W_1 is the total length of interdigital part, W_3 is the length of finger, and n is the number of fingers. From (1b), it can be seen that the parameter Ci has an effect on the second resonant frequency but has little effect on the fundamental frequency due to (1a). This can be explained by the fact that Ci can shift the second resonant frequency and reduce an electrical length of the resonator in unit cell to around $\lambda/4$. Additionally, with
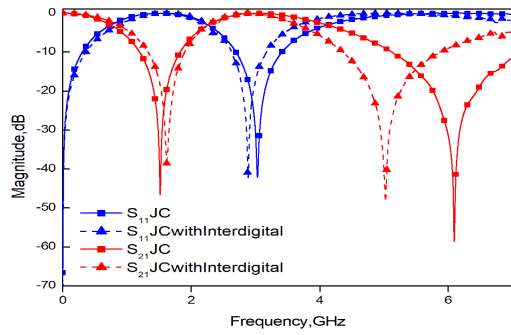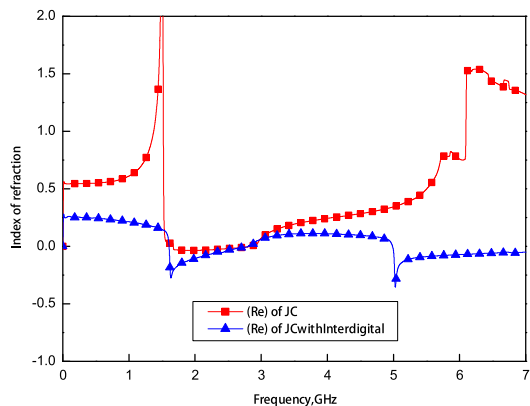
(a)
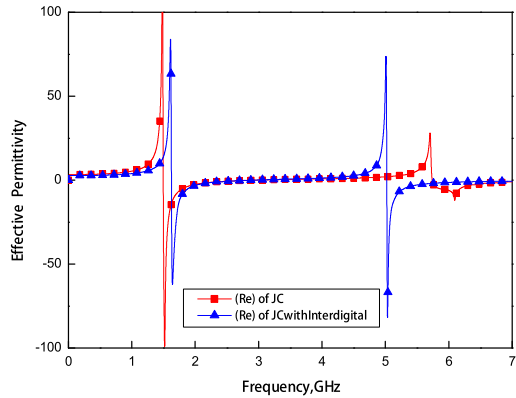
(b)
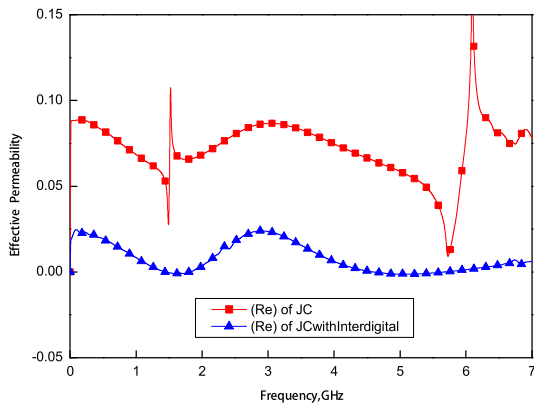
(c)

(d)

FIGURE 3. The simulation result of (a) the S-parameters, (b) the effective permittivity, (c) the effective permeability, and (d) the index of refraction.
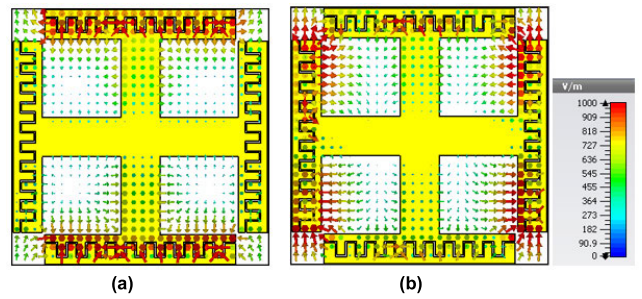

FIGURE 4. The E-field of Jerusalem cross structure with Interdigital at (a) 1.8 GHz, and (b) 5.5 GHz.
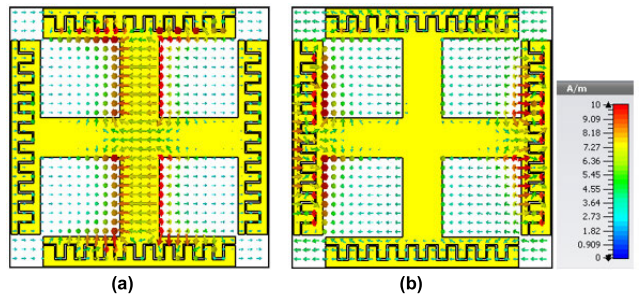

FIGURE 5. The H-field of Jerusalem cross structure with Interdigital part at (a) 1.8 GHz, and (b) 5.5 GHz.
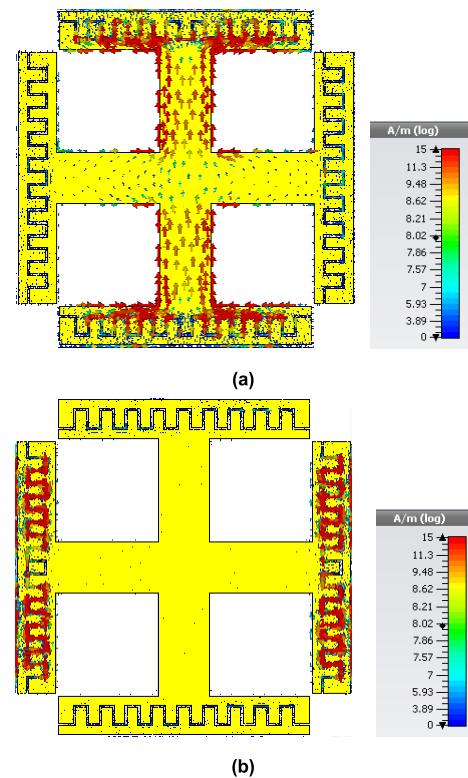

(a)

(b)

FIGURE 6. The surface current of unit cell at (a) 1.8 GHz, and (b) 5.5 GHz.

the proposed unit cell structure, its permittivity could be flexibly adjusted. In the boundary condition, the direction of propagation (k) and the E-H field are in z direction and y-x axis, respectively. To analyze the characteristics of the
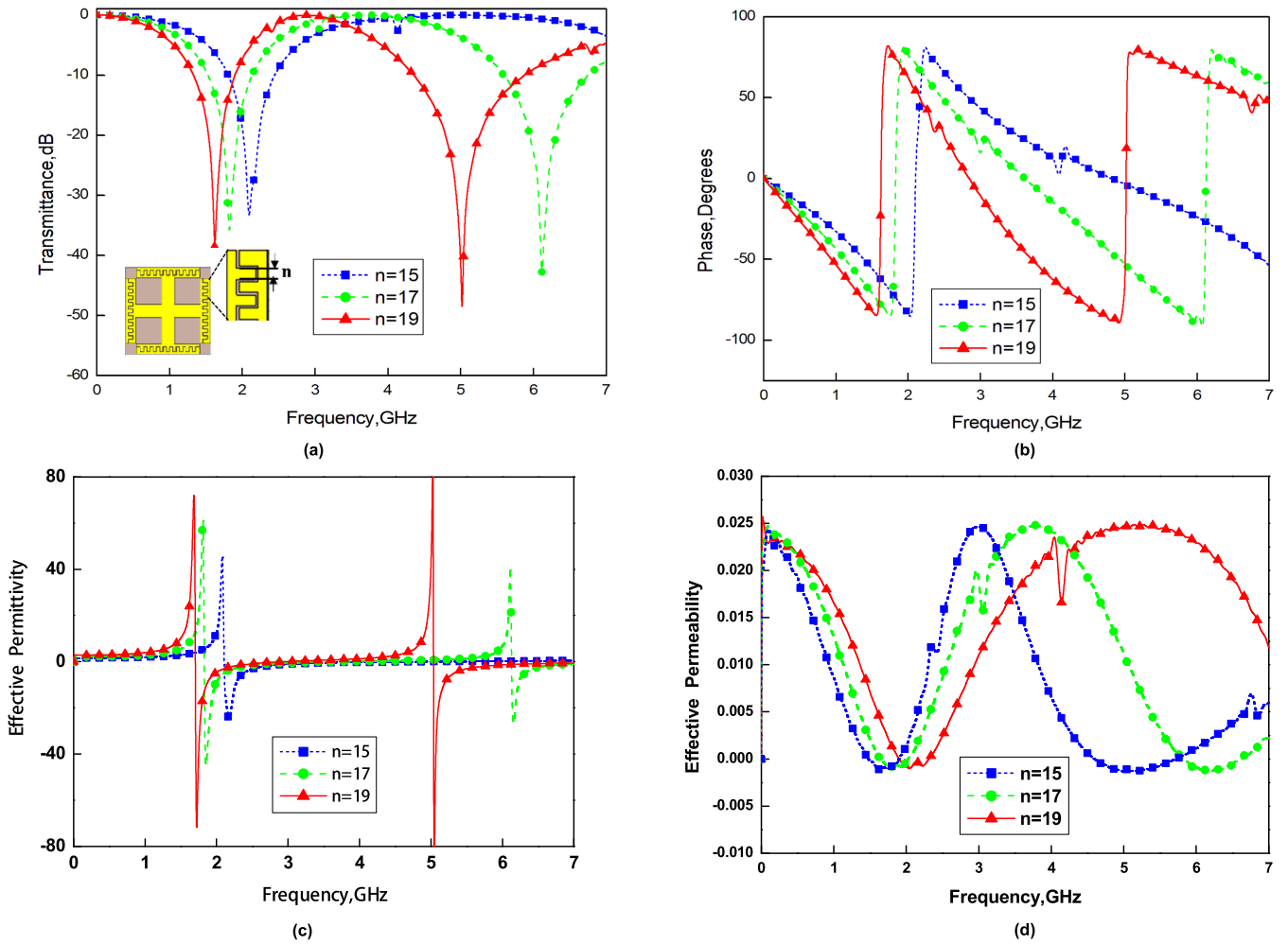
FIGURE 7. The simulation results of (a) the magnitude of (S$_{21}$), (b) the phase of S$_{21}$, (c) the effective permittivity, and (d) the effective permeability.

metamaterial structure, the S-parameters are extracted to calculate the effective permittivity (ε_{eff}), and permeability (μ_{eff}) that are derived as follows [26]–[28],

$$\text{Effective permittivity, } \varepsilon_r = \left(\frac{2}{jkd}\right) \times \left[\frac{1-(S_{21}+S_{11})}{1+(S_{21}+S_{11})}\right] \quad (3)$$

$$\text{Effective permeability, } \mu_r = \left(\frac{2}{jkd}\right) \times \left[\frac{1-(S_{21}-S_{11})}{1+(S_{21}-S_{11})}\right] \quad (4)$$

where k is the wave number, d is the thickness of substrate, S$_{11}$ is reflection coefficient, and S$_{21}$ is transmission coefficient. By using the CST simulation software, which is based on the finite-element method, the geometrical parameters of W$_1$, W$_2$, W$_3$, W$_4$, W$_5$, W$_6$ and g$_1$ are obtained to be 22.53 mm, 0.94 m, 1.66 mm, 3.47 mm, 4.60 mm, 23.04 and 0.20 mm, respectively. The overall size of unit cell is 3.0 × 3.0 cm^2, which is more compact compared to the conventional structure as shown in Fig. 2(b).

## III. RESULTS AND DISCUSSION

A. METAMATERIAL UNIT CELL

Fig. 3(a) displays the simulated results of the conventional Jerusalem structure compared to the proposed structure. It is

found that the combination of Jerusalem cross structure and interdigital part can control obviously the second resonant frequency but affect little the first resonant frequency and also change the value of material properties as shown in Fig. 3(b)-(d). In Figs. 4(a) and (b), the E-field occurs in the y-axis at the resonant frequency of 1.8 GHz and the intensity of the E-field is higher than the second resonant frequency of 5.5 GHz. In the case of the x-axis, the intensity of the E-field at the resonant frequency of 1.8 GHz is less than the second resonant frequency of 5.5 GHz but the H-field hardly appears during interdigital part at both resonant frequencies of 1.8 GHz and 5.5 GHz. as shown Figs. 5(a). and (b).

For better illustration about the structure that affected the resonance frequency using interdigital technique, the surface currents at both resonance frequencies are displayed in Figs. 6(a) and (b). Fig. 7 displays the simulated results of the proposed structure to apprehend change of the capacitance according to the number n of interdigital part, causing the shift of the resonant frequencies, especially the second resonant frequency. In Fig. 7(a), at n = 19, the consequence from the simulation found that there are resonant frequencies
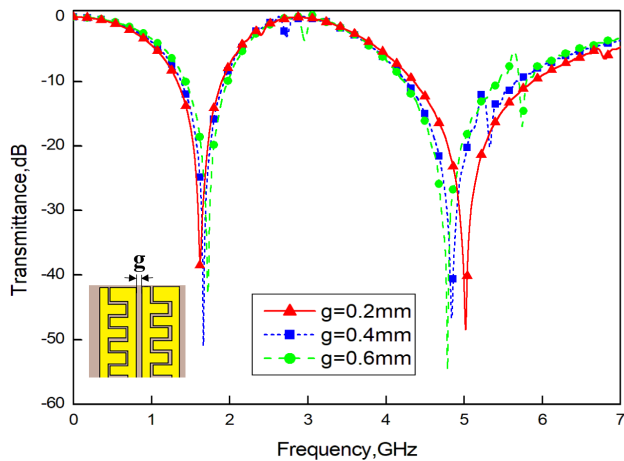
(a)
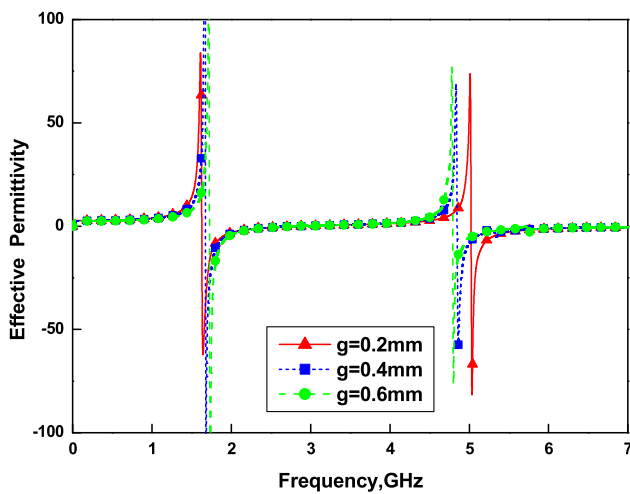
(b)

FIGURE 8. The simulation results of (a) the magnitude of (S$_{21}$), and (b) the effective permittivity.

FIGURE 9. The E-field of Jerusalem cross structure with interdigital part at (a) 1.8 GHz, and (b) 5.5 GHz.

FIGURE 10. The E-field of conventional Jerusalem cross structure at (a) 1.8 GHz, and (b) 5.5 GHz.
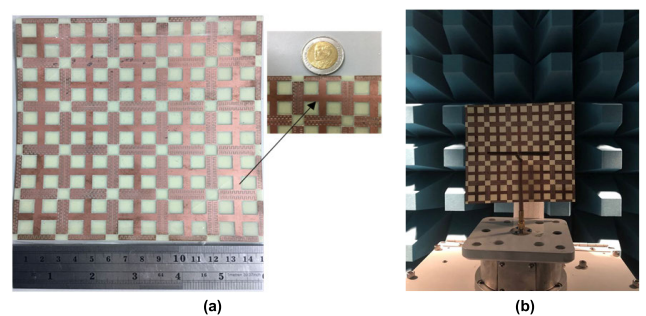
FIGURE 11. Photos of (a) the proposed metamaterial, and (b) the measurement set-up.

of 1.8 GHz and 5.5 GHz by the observation from transmission coefficient (S$_{21}$) that covers the bands of 1.8 GHz and 5.5 GHz, respectively as designed. In addition, the conjugation of Jerusalem cross structure and interdigital part affects especially to the density of E-field, resulting in the value of permittivity change plentifully but it has inappreciable effect on H-field. Moreover, the negative permittivities are achieved at both frequency ranges. The first one is approximately from 1.70 to 1.95 GHz, while the second one is from 5.06 to 6.04 GHz as shown in Fig. 7(c). The permeability values of both frequencies are near zero as shown in Fig. 7(d). In addition, the gap between the unit cells also affects the coupling between the unit cells, causing the resonant frequencies to be slightly shifted as shown in Fig. 8.

Using interdigital technique results in the intensity of E-field between gaps of the interdigital. At the resonant frequency of 1.8 GHz, the intensity of E-field is the most occurring in the gap between the unit cell and the second most occurring in gaps of the interdigital part as shown in Fig. 9(a). At the second resonant frequency of 5.5 GHz,
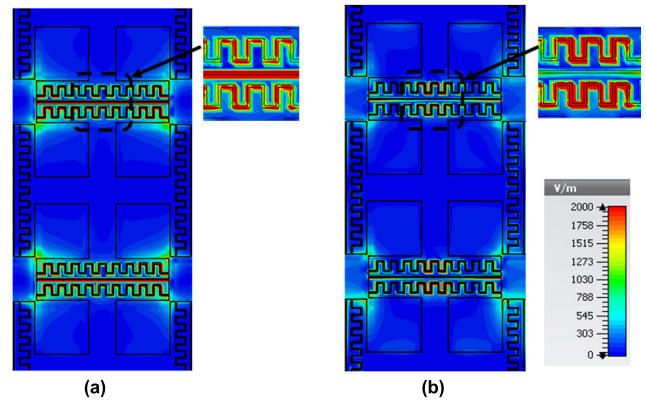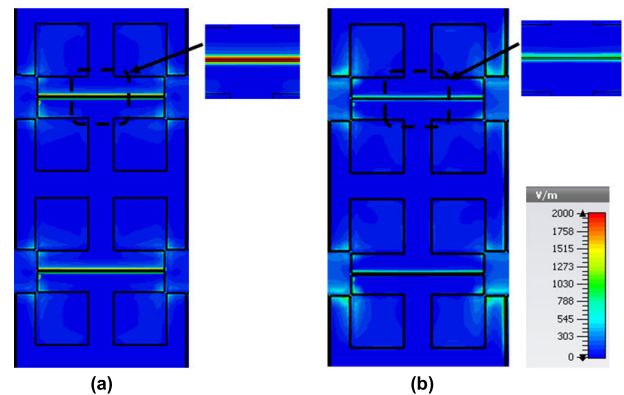
the intensity of E-field appears at the gaps of the interdigital part, obviously as shown in Fig. 9(b). It can be compared with the E-field of the conventional Jerusalem cross structure as shown in Fig. 10, in which the permittivity of material can be adjusted by using interdigital technique with Jerusalem cross structure.

B. METAMATERIAL WITH ANTENNA
Figs. 11(a) and (b) present the proposed metamaterial and the measurement setup. The proposed metamaterial with a size

(a)

(b)

FIGURE 12. The measured and simulated results (S$_{11}$) of the dipole antennas at (a) 1.8 GHz, and (b) 5.5 GHz.

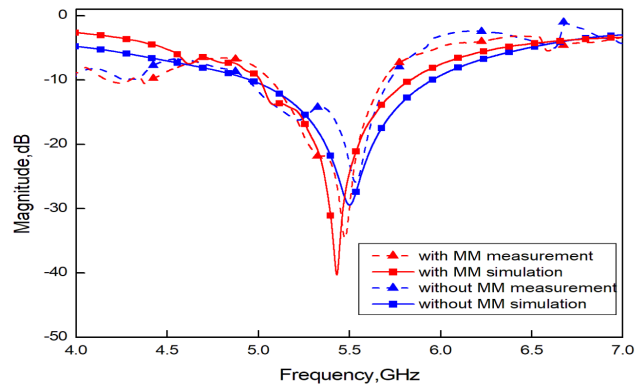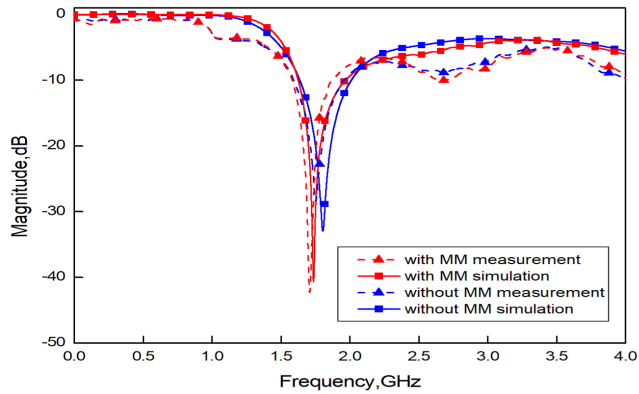**FIGURE 13.** The radiation patterns of V-polarization at (a) 1.8 GHz, and (b) 5.5 GHz.

(a)

(b)

FIGURE 14. The radiation patterns of H-polarization at (a) 1.8 GHz, and (b) 5.5 GHz.

(a)

(b)

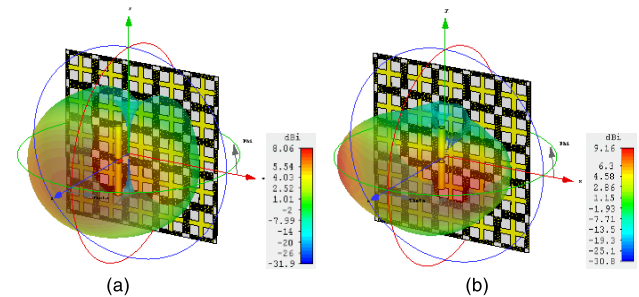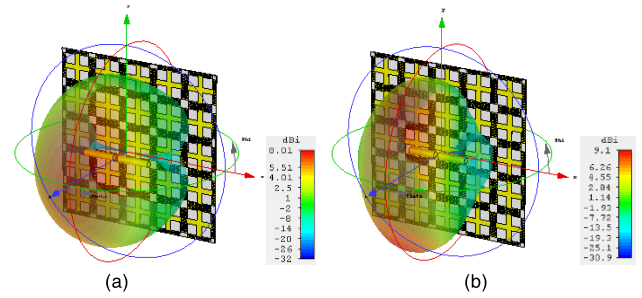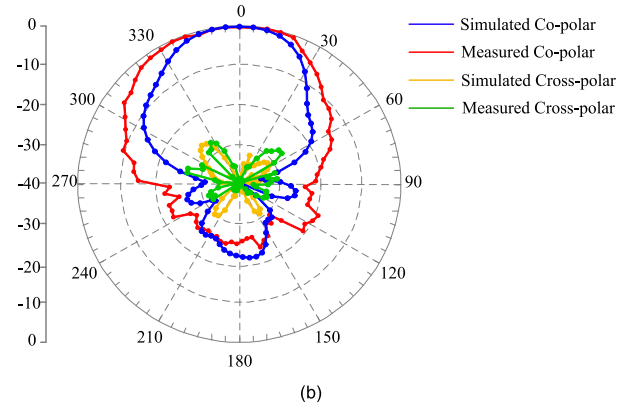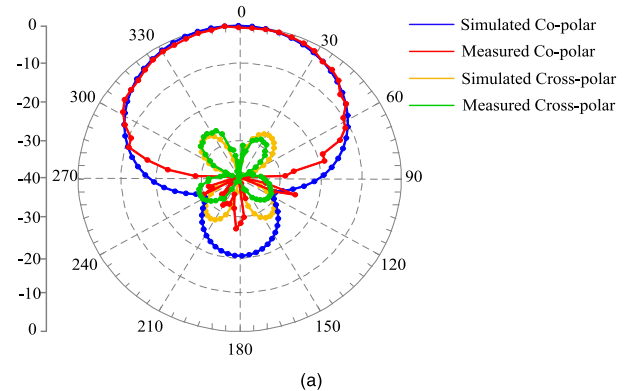**FIGURE 15.** The E-plane radiation patterns at (a) 1.8 GHz, and (b) 5.5 GHz.

of the 15×15 cm^2 was fabricated. In this setup, a dipole antenna was employed with the proposed metamaterial as a reflector. The proposed metamaterial was placed on a holder at a proper distance of 2.0 cm or about one-eighth wavelength behind the dipole antenna. Another identical dipole was used as a receiving antenna. Both dipole antennas were connected to a network analyzer in an anechoic chamber.

Fig. 12 demonstrates the simulated results of the dipole antenna with the proposed metamaterial exhibiting the resonance ranges at 1.74 GHz (1.64 $\sim$ 1.97 GHz) and 5.43 GHz (5.01 $\sim$ 5.83 GHz) as well as the measured resonance ranges are 1.71 GHz (1.58 $\sim$ 1.88 GHz), 5.47 GHz (5.05 $\sim$ 5.68 GHz), respectively. It can be compared with

the dipole antenna ranges at 1.80 GHz (1.63 $\sim$ 2.00 GHz) and 5.50 GHz (4.96 $\sim$ 5.95 GHz) in simulation as well as 1.75 GHz (1.59 $\sim$ 1.96 GHz), 5.52 GHz (4.95 $\sim$ 5.71 GHz) in measurement. The resonant frequencies are shifted toward the lower frequency, which the measured return losses (S$_{11}$) of the proposed metamaterial are -46.45, and -37.16 dB, respectively compared with -29.83 and -26.20 dB of the dipole antenna. Therefore, the proposed dual-band metamaterial is applicable for LTE and WLAN applications. The measured and simulated peak gains of the antenna by using the Friis transmission formula at 1.8 GHz and 5.5 GHz are good agreement. The measured gains of the antenna increase up to 8.23 dBi and 8.30 dBi, respectively, whereas the simulated gains are sequentially 8.06 dBi and 9.16 dBi as shown in Figs. 13 and 14. Figs. 15 and 16 show the

FIGURE 16. The H-plane radiation patterns at (a) 1.8 GHz, and (b) 5.5 GHz.

comparison between measured and simulated far-field radiation patterns in E-plane and H-plane of vertical polarization at the resonant frequencies. In the cas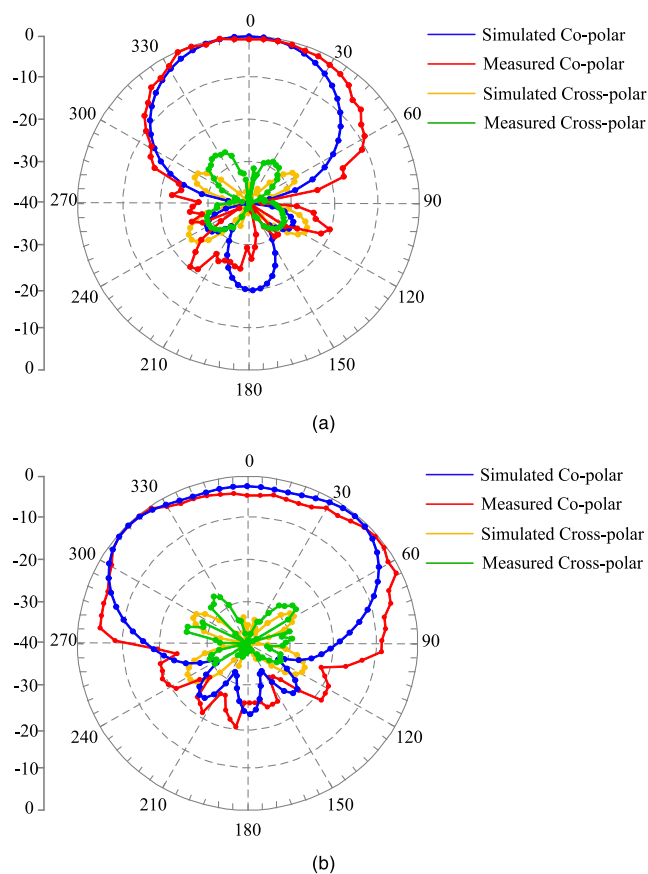e of vertical polarization, the yz-coordinates are taken into consideration as E-plane and xz-coordinates as H-plane. For horizontal polarization, the yz and xz-coordinates are just switched for E-plane and H-plane, which can be examined that the proposed metamaterial to lead to dual linear polarization, resulting in ease of use with the antennas. In addition, the co-polarization is greater than the cross-polarization at both resonant frequencies due to the use of interdigital technique in conjunction with Jerusalem cross structure. When comparing with [7]–[9], using the proposed technique, the size of unit cell is smaller because it can be reduced from λ/2 to λ/4 caused by the slow wave effect on transmission line. When connecting with the antenna, the proposed reflector can be used to reflect the waves in both E and H planes or dual polarization and the antenna also has higher gains at both frequencies. In addition, the proposed design technique was done in a single layer, which is less complicated compared with the reported works. When comparing with the Jerusalem structure proposed in [12]–[14], even though it can control the second harmonics resulting in a dual band operation by using difference of impedance in a cross transmission line but the size of unit cell is quite large and the antenna with this proposed reflector has low gain about 6 dB.

IV. CONCLUSION

In conclusion, a dual-band metamaterial based on Jerusalem cross structure with interdigital technique has been designed, fabricated and measured in this paper. The unit cell and array structure exhibited negative permittivity (ENG) at 1.8 GHz (1.70 ~ 1.95 GHz) and 5.5 GHz (5.06 ~ 6.04 GHz). The dipole antenna has been used with the proposed metamaterial and also operated with dual linear polarization for simulation purposes to obtain good agreement in the measured results. The advantage of the proposed metamaterial reflector includes small size of unit cell about one-fourth wavelength at 1.8 GHz, that can be used for dual-band frequency operation. Also, the dipole can be placed in two directions (x or y direction), resulting in the same radiation patterns. The distance between radiator and metamaterial reflector is reduced to about one-eighth wavelength. The dipole antenna with the proposed metamaterial reflector has simulated gains up to 8.16 dBi and 9.06 dBi and measured stable gains up to 8.23 dBi and 8.30 dBi at both frequencies. In addition, the purposed metamaterial is applicable for 4G LTE, and WLAN systems.

REFERENCES

[1] S. E. Mendhe and Y. P. Kosta, "Metamaterial properties and applications," *Int. J. Inf. Technol. Knowl. Manag.*, vol. 4, no. 1, pp. 85–89, 2011.

[2] S. Chaimool, and P. Akkaraekthalin, "Metamaterials for antenna applications," *J. KMUTNB*, vol. 21, no. 2, pp. 472–482, May 2011.

[3] P. Moitra, B. A. Slovick, W. Li, I. I. Kravchenko, D. P. Briggs, S. Krishnamurthy, and J. Valentine, "Large-scale all-dielectric metamaterial perfect reflectors," *ACS Photon.*, vol. 2, no. 6, pp. 692–698, Jun. 2015.

[4] S. Ahdi Rezaeieh, M. A. Antoniades, and A. M. Abbosh, "Bandwidth and directivity enhancement of loop antenna by nonperiodic distribution of Mu-negative metamaterial unit cells," *IEEE Trans. Antennas Propag.*, vol. 64, no. 8, pp. 3319–3329, Aug. 2016.

[5] Y. Tian, G. Wen, and Y. Huang, "Multiband negative permittivity metamaterials and absorbers," *Adv. Opto Electron.*, vol. 2013, pp. 1–7, 2013.

[6] S. Enoch, G. Tayeb, P. Sabouroux, N. Guérin, and P. Vincent, "A metamaterial for directive emission," *Phys. Rev. Lett.*, vol. 89, no. 21, 2002, Art. no. 213902.

[7] Y. Ma, Q. Chen, J. Grant, S. C. Saha, A. Khalid, and D. R. S. Cumming, "A terahertz polarization insensitive dual band metamaterial absorber," *Opt. Lett.*, vol. 36, no. 6, p. 945, Mar. 2011.

[8] Z. Qu, Y. Zhang, and B. Zhang, "Double square rings with different dimensions produce multiple absorption bands," *Appl. Opt.*, vol. 58, no. 1, p. 152, Jan. 2019.

[9] M. Bahadorzadeh and C. F. Bunting, "A dual band-reject FSS for WI-FI application," in *Proc. Int. Appl. Comput. Electromagn. Soc. Symp. (ACES)*, Mar. 2018, pp. 1–2.

[10] D. Marathe and K. Kulat, "A compact triple-band negative permittivity metamaterial for C, X-band applications," *Int. J. Antennas Propag.*, vol. 2017, pp. 1–12, 2017.

[11] H. V. H. S. Filho, C. P. N. Silva, M. R. T. D. Oliveira, E. M. F. D. Oliveira, M. T. D. Melo, T. R. D. Sousa, and A. G. Neto, "Multiband FSS with fractal characteristic based on jerusalem cross geometry," *J. Microw.* Optoelectron. Electromagn. Appl., vol. 16, no. 4, pp. 932–941, Dec. 2017.

[12] F. S. Jafari, M. Naderi, A. Hatami, and F. B. Zarrabi, "Microwave Jerusalem cross absorber by metamaterial split ring resonator load to obtain polarization independence with triple band application," *AEU Int. J. Electron. Commun.*, vol. 101, pp. 138–144, Mar. 2019.

[13] S. Wang, J. Gao, X. Cao, J. Lan, and Z. Huang, "Integrated Radiation and Scattering Performance of Metasurface Antenna Array," in *Proc. Int. Conf. Microw. Millim. Wave Technol. (ICMMT)*, May 2018, pp. 1–3.

[14] J. J. Liu, Y. J. Chen, N. Xu, Y. H. Ren, G. X. Xu, C. L. Ji, Z. Y. Zhao, Y. Y. Zhang, and R. P. Liu, "A multi-mode cavity filter with Jerusalem Cross structure resonator," in *Proc. Asia–Pacific Microw. Conf. (APMC)*, Nov. 2013, pp. 887–889.

[15] B. Belyaev, A. M. Serzhantov, A. A. Leksikov, Y. F. Bal'va, and A. A. Leksikov, "High-quality compact interdigital microstrip resonator and its application to bandpass filter," *Pier C*, vol. 72, pp. 91–103, Oct. 2017.

[16] X. Zhang, Y. Wen, and K. Zhou, "A capacitive loaded quasi-elliptic function microstrip filter on GSM-R band," in *Proc. 3rd IEEE Int. Symp. Microw., Antenna, Propag. EMC Technol. Wireless Commun.*, Oct. 2009, pp. 535–537.

[17] *Overview on Interdigital Capacitor Design*, Agilent Technol., Santa Clara, CA, USA, 2001, p. 10.

[18] J. Gu, F. Zhang, C. Wang, Z. Zhang, M. Qi, and X. Sun, "Miniaturization and harmonic suppression open-loop resonator bandpass filter with capacitive terminations," in *IEEE MTT-S Int. Microw. Symp. Dig.*, Jun. 2006, pp. 373–376.

[19] J. Hong and M. Lancaster, "End-coupled microstrip slow-wave resonator filter," *Electron. Lett.*, vol. 32, no. 16, p. 1494, 1996.

[20] N. Engheta, "Metamaterials with negative permittivity and permeability: Background, salient features, and new trends," in *IEEE MTT-S Int. Microw. Symp. Dig.*, vol. 1, Aug. 2003, pp. 187–190.

[21] H. R. Stuart, "The application of negative permittivity materials and metamaterials in electrically small antennas," in *Proc. IEEE Antennas Propag. Soc. Int. Symp.*, vol. 1, Jun. 2007, pp. 1–6.

[22] P. Chomtong and P. Akkaraekthalin, "A quad-band bandpass filter using stepped impedance resonators with interdigital capacitors," *IEEJ Trans. Elect. Electron. Eng.*, vol. 13, no. 8, pp. 1080–1086, Aug. 2018.

[23] S. Meesomklin, P. Chomtong, and P. Akkaraekthalin, "A compact multiband BPF using step-impedance resonators with interdigital capacitors," *Radio Eng.*, vol. 25, no. 2, pp. 258–267, Apr. 2016.

[24] P. Chomtong and P. Akkaraekthalin, "A triple-band bandpass filter using Tri-section step-impedance and capacitively loaded step-impedance resonators for GSM, WiMAX, and WLAN systems," *Frequenz*, vol. 68, nos. 5–6, pp. 227–234, 2014.

[25] P. Chomtong, C. Mahatthanajatuphat, and P. Akkaraekthalin, "A dual-band band-pass filter with overlap step-impedance and capacitively loaded hairpin resonators for wireless LAN systems," *Int. J. Microw. Sci. Technol.*, vol. 2011, pp. 1–9, May 2011.

[26] J. Manuel and T. Alves, "Metamaterials with negative permeability and permittivity: Analysis and application," M.S. thesis Universidade Tecnica de Lisboa Instituto Superior Tecnico, Lisbon, Portugal, Oct. 2010.

[27] D. Smith, S. Schultz, P. Markoš, and C. Soukoulis, "Determination of negative permittivity and permeability of metamaterials from reflection and transmission coefficients," *Phys. Rev. B, Condens. Matter*, vol. 65, pp. 1–5, Nov. 2001.

[28] X. Chen, T. M. Grzegorczyk, B.-I. Wu, J. Pacheco, Jr., and J. A. Kong, "Robust method to retrieve the constitutive effective parameters of metamaterials," *Phys. Rev. E, Stat. Phys. Plasmas Fluids Relat. Interdiscip. Top.*, vol. 70, no. 1, 2004, Art. no. 016608.

W. KAMONSIN received the B.Eng. degree in telecommunication engineering from the Suranaree University of Technology (SUT), Nakhon Ratchasima, Thailand, in 2017, where he is currently pursuing the M.S. degree in telecommunication engineering.

P. KRACHODNOK (Member, IEEE) received the D.Eng. and Ph.D. degrees in telecommunication engineering from the Suranaree University of Technology (SUT), Thailand, in 2008, where he has been working for 11 years. His experience and expertise are in electromagnetic theory, microwave engineering, and antenna engineering.

P. CHOMTONG (Member, IEEE) received the M.Eng. and Ph.D. degrees in electrical engineering from the King Mongkut's University of Technology North Bangkok (KMUTNB), Thailand, in 2006 and 2011, respectively. In 2012, he joined the Department of Teacher Training in Electrical Engineering, KMUTNB, as an Instructor. His current research interests include passive and active microwave circuits, wideband and multiband antennas, and telecommunication systems.

P. AKKARAEKTHALIN (Member, IEEE) received the B.Eng. and M.Eng. degrees in electrical engineering from the King Mongkut's University of Technology North Bangkok (KMUTNB), Thailand, in 1986 and 1990, respectively, and the Ph.D. degree from the University of Delaware, Newark, USA, in 1998. From 1986 to 1988, he worked at Microtek Laboratories, Thailand. In 1988, he joined the Department of Electrical Engineering, KMUTNB. His current research interests include passive and active microwave circuits, wideband and multiband antennas, and telecommunication systems. He is a member of IEICE Japan and ECTI Thailand. He was the Chairman for the IEEE MTT/AP/ED Thailand Joint Chapter, from 2007 to 2008, and the President of ECTI Association, from 2014 to 2015. He is the Head of the Senior Research Scholar Project of Thailand Research Fund (TRF).

• • •